Digital Image Plane Holography (DIPH) for two-phase flow diagnostics in multiple planes

V. Palero, J. Lobera and M. P. Arroyo
Dpto. Física Aplicada. Facultad de Ciencias. Universidad de Zaragoza
C/ Pedro Cerbuna, 12, 50009 – Zaragoza. SPAIN
e-mail: palero@unizar.es
Tel. +34 976 762691   Fax. +34 976 761233

ABSTRACT

In this paper the size and displacement of air bubbles in glycerine are measured in two planes. Digital Image Plane Holography (DIPH) is used for the simultaneous recording of both planes (figure1). A new optical configuration is introduced for illumination. A fluid plane is illuminated with two laser sheets propagating in two opposite directions. The defocused image fields are holographically recorded at 90º. The two image fields are independently reconstructed. The bubble fields are recovered either in a defocused plane (figure 2a,b) or in the best-focused plane (figure 2c,d). The analysis of the images in a defocused plane provides the bubbles sizes while the cross-correlation of the focused images provides the velocity field, as in a regular PIV experiment. In these experiments the free movement of air bubbles in glycerine has been studied. Bubbles diameters from 50 μm to 400 μm and displacements up to 300 μm have been obtained.
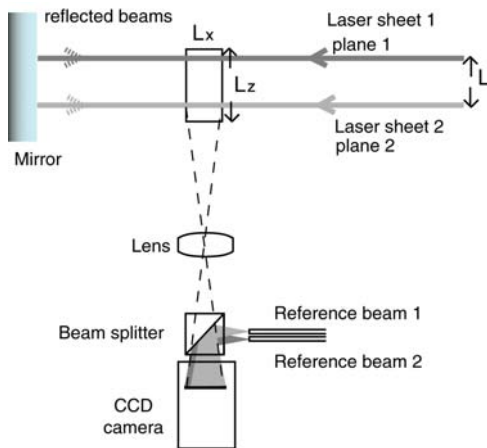
Figure 1: 3-D DIPH optical set-up for a multiplexed recording of two fluid planes
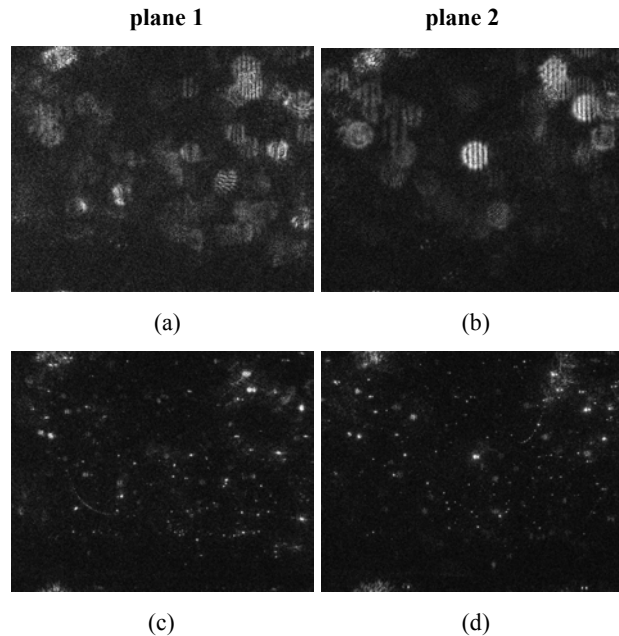

Figure 2: Reconstructed images: Defocused images for plane 1 (a) and 2 (b) as they are imaged in the CCD sensor in the hologram recording; Focused images for plane 1 (c) and plane 2 (d).

Introduction

The experimental diagnostics of two-phase flows usually involves a simultaneous measurement of size and velocity of the disperse phase. The measurement of the size from features that are intensity independent is highly convenient, as the measured sizes will not depend on the laser beam intensity or obscuration. A first approach for transparent droplets was proposed by Glover et al. (1995). If a fluid plane is illuminated with a laser sheet, each of the transparent droplets immersed in the laser sheet will scatter light that is refracted and reflected thus yielding either a fringe pattern (defocused particle image) or two distinctive spots (focused particle image). The fringe count or fringe frequency and the separation between the two spots provide the droplet size. Glover et al. (1995) developed a technique, called interferometric laser imaging for droplet sizing (ILIDS) in sparse polydisperse sprays. It is based on the photographic recording of the far field fringe pattern associated to each droplet. This ILIDS technique has been later applied with different modifications by Maeda et al. (2000) and Burke et al. (2002). Burke et al. (2002) introduced a digital holographic recording where the object and reference wavefronts are recorded on a CCD sensor. From the captured intensity pattern (digital hologram) the diffracted wavefront can be later reconstructed mathematically. Because of the three-dimensional capability of holography, the calculated wavefront can be chosen to show either the fringe pattern or the two spots.

Burke et al. (2002) used a digital image plane holographic (DIPH) set-up where the (defocused) particle image field is formed on the CCD sensor and a collimated beam is used as the reference. DIPH with focused particle image field and a divergent reference beam has already been used in our laboratory (Lobera et al., 2003) for the measurement of the 3-C velocity field in a convective flow. We have shown that this holographic set-up, which produces a lensless Fourier transform hologram of the imaging lens aperture, not only allows an easy isolation of the real image term from the virtual and the dc terms, but it also allows a simultaneous recording but independent reconstruction of multiple fluid planes, with an appropriated coherence length matching of the reference and object waves corresponding to each plane. Here we propose to apply this multiple plane DIPH to defocused particle image fields for particle size and displacement measurement in a quasi 3-D region.

2. Experimental set-up and hologram recording

DIPH has its origin in the spatial phase shifting-digital speckle pattern interferometry (SPS-DSPI), a technique used in solid mechanics, but reported quite recently as a velocimetry technique (Lobera et al, 2003).

A fluid plane is illuminated with a laser sheet and a lens is used to image the object onto the CCD sensor. Specific of this DPIH set-up is the divergent reference beam that has to be placed in a very precise position respect to the object beam. The reference beam has to originate in the same plane and at a suitable distance form the lens aperture. A beam splitter placed between the lens and the CCD camera sensor combines the reference and object beams (figure 1).

The hologram recorded by the CCD sensor contains information on the amplitude and phase of both the object and the reference beams, and can be expressed as:

$$I = I_o + I_r + 2\sqrt{I_o I_r} \cos(\phi_o - \phi_r) \qquad (1)$$

where I and ϕ are the intensity and phase, with o and r referring to the object and the reference waves. Let us note that ϕ_o is a spatially random phase as it changes from one particle to the next. This ϕ_o needs to be locally constant in a 2-3 pixel area in order for the CCD sensor to be able of recording the spatial frequencies associated to the hologram recording. Thus, the lens aperture is chosen to ensure a minimum speckle size of 3 pixels. This requirement is common to digital PIV for an appropriate accuracy.

DIPH is a 3-D technique. Although a whole volume could be illuminated, a much better use of the laser energy and much less noise from defocused particle images is obtained with a multiple light-sheet illumination. Thus much bigger volumes with higher particle concentrations can be recorded with the appropriate sampling by properly selecting the light sheet geometry (Lobera et al, 2004). Several holographic recordings can be fractally multiplexed by using reference beams with point sources in different position for each recording and taking advantage of the beam temporal coherence length properties. This means that each reference beam has to be made coherent with only one fluid plane.

For the present experiments a Spectron Nd:YAG pulsed laser ($\lambda = 0.532$ μm) was used for illumination. The light beam is divided into an object and a reference beams. Each of them is also subdivided in two (figure 1). Two light sheets separated L = 18.5 mm, illuminated a plexiglass rectangular cell (Lx = 14,6 mm; Ly = 12.5 mm; Lz= 25 mm) filled with glycerine (n= 1.475). Air bubbles were injected inside the cell with a syringe. A Nikkor AM ED f=120 mm, working at f#19, acquires the light scattered by the bubbles, that interferes with two reference beams in the CCD sensor of a PCO camera (12 bits, 1280Hx1024V, 6.7 μm/pixel). The visualized area covers 12.1mm x 9.7mm in plane 1 and 11.1mm x 8.9mm in plane 2. The corresponding magnifications are M_1= 0.71 and M_2 = 0.77. The two reference beams passed through two optical fibres, whose ends are at the same distance from the CCD plane than the lens aperture.

The defocused image field is recorded, as in a regular ILIDS experiment, but adding a reference beam. In this case the CCD sensor was located between the lens and the best-focused plane. The position of the camera will be also determined by the scattering angle that provides the best fringe contrast in the defocused particle images. However, an angle of recording of 90º is most suitable, especially if a combination with PIV is desired for measuring velocity and size simultaneously or if the recording camera and the particles are not immersed in the same medium, as in our case. For relative refractive indexes smaller than unity, the limiting condition for the scattering angle from geometrical optics corresponds to total reflection on the first surface of the bubble, given by:

$$\theta_s = 2 \arccos(m) \qquad (2)$$

where θ_s is the scattering angle, and m is the relative refractive index (n_2/n_1).

For air bubbles in glycerine the maximum scattering angle would be 94.6º. But, Semidetnov and Tropea (2004) have shown that at the maximum scattering angle the glare point for first-order refraction coincides with the glare point for the reflection and therefore the ILIDS arrangement is impractical for scattering angles close to the maximum allowed scattering angle.

A different approach can be done using an arrangement similar to the global phase Doppler technique (Damaschke et al, 2001), i.e., by illuminating the particle field with two light sheets. An easy way to create a second illuminating sheet is by putting a mirror after the fluid, so the "new" light sheet is propagating in the opposite direction to the first one (figure 1). Special care has to be taken in positioning the mirror. It has to be adjusted at an appropriate distance in order to keep the coherence between the point sources and the reference beam, and has to be perfectly perpendicular to the original illumination sheet. Therefore, the glare points in the surface of the sphere will correspond to the first reflection of each sheet. Their intensity will be the same and the contrast of the fringes will be optimum. Besides, this configuration can be used with opaque reflective particles as no refraction is involved. In figure 3 an example of the defocused bubbles recorded with (figure 3a) and without mirror (figure 3b) is shown. Two planes have been recorded simultaneously (f#= 2.8), with different degree of defocusing, as can be seen by the sizes of the defocused images. The bigger images correspond to the bubbles in plane 2 while the smaller images are bubbles in plane 1.

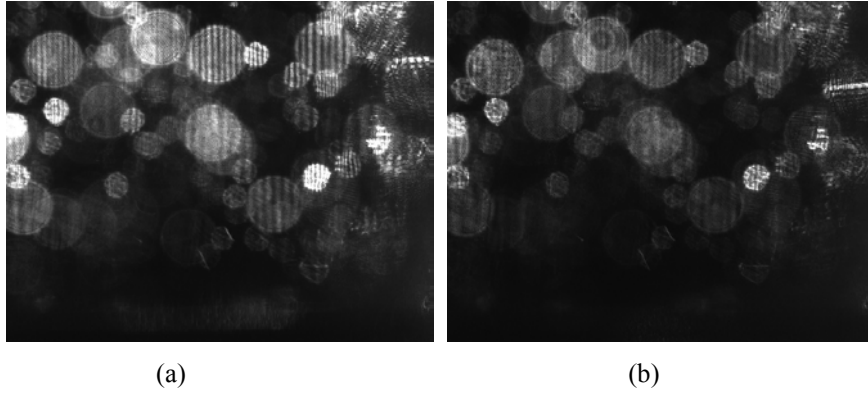(a)   (b)

Figure 3: Defocused particle images a) with a mirror located after the fluid; b) without a mirror.
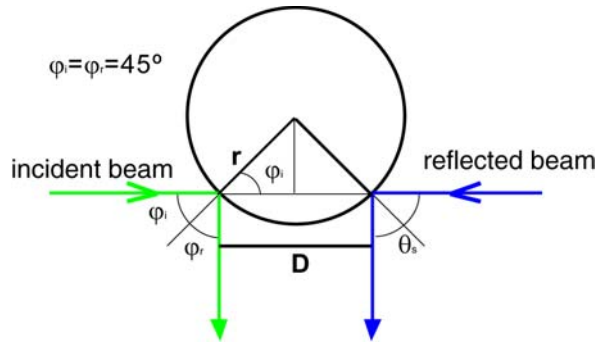

Figure 4: Incident and reflected beam paths in the bubble

Now, the relation that gives the bubble diameter from the distance between glare points has to be calculated. We can consider each glare point on the surface of the particle as a point source of a spherical wave propagating towards the detector. Then the fringe pattern of the defocused particle image can be studied as arising from the interference between two coherent point sources, like in the Young's fringe experiment. Therefore, the fringe spacing Δy is given by:

$$\Delta y = \frac{\lambda z}{D} = z\Delta\varphi \qquad (3)$$

where λ is the illumination wavelength, z is the distance between the point sources and the recording plane, D is the distance between the glare points and Δφ is the angular fringe spacing. In this particular case D can be calculated as indicated in figure 4:

$$D = 2rM\cos 45 \qquad (4)$$

where r is the bubble radius and M is the magnification in each plane. Then the diameter d of the bubble can be calculated from the angular fringe spacing as:

$$d = \frac{\lambda}{M\Delta\varphi\cos 45} \qquad (5)$$

A more common way to express the diameter bubble is considering the number of the recorded interference fringes and the parameters of the optical system. Then, the bubble diameter can be expressed as:

$$d = \frac{N\lambda f\#}{\cos 45}\frac{(1+M)}{M} \qquad (6)$$

where N is the number of fringes and f# is the aperture number. With the present configuration two holograms of two planes are recorded simultaneously. Figure 5 shows an example of a hologram acquired with this set-up.
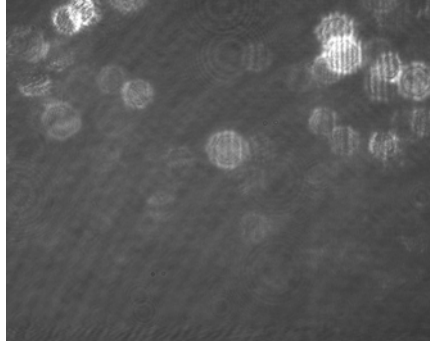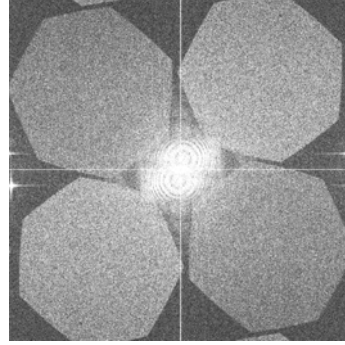

Figure 5: Digital hologram   Figure 6: Frequency power spectrum

3. Analysis of the digital holograms

In digital holography the most common reconstruction process is similar to optical holography: the hologram intensity is multiplied by the reference or its conjugated beam and the output wave is propagated back to either the real or the virtual image plane. With our recording set-up each of the multiplexed holograms behaves as a lensless Fourier hologram of the lens aperture. The frequency power spectrum of the recording shows this (figure 6). In figure 6 the real and virtual images of the lens aperture for each hologram are completely separated. Each pair of heptagons along the two diagonals is the real

and virtual images of the lens aperture for each hologram. Here, the need for limiting the lens aperture so the particle size will be 3 pixels can be also seen.

The numerical reconstruction is done using the Rayleigh-Sommerfeld diffraction. (Lobera et al., 2004). Firstly, the hologram is multiplied by a numerical wave equivalent to the conjugated of the reference wave, $r*(x,y)$ (figure 7a). Then, the reconstructed wave is propagated from the sensor plane to the aperture plane, where the virtual image of the corresponding plane is selected, and from there, the reconstructed wave is propagated again to the plane of interest (figure 7b).

The process for recovering the bubble size is described below. Once a particle is selected in the focused plane, the rest of the wave is set at zero. This wave is propagated to the aperture plane, where the high frequencies introduced by the cutting in the initial image are filtered out (figure 7c). Again, the wavefront is propagated to the sensor (defocused) plane, where the Fourier transform of the intensity is calculated. The result is the autocorrelation function of the focused image from where the fringe spacing (Δy) can be obtained.
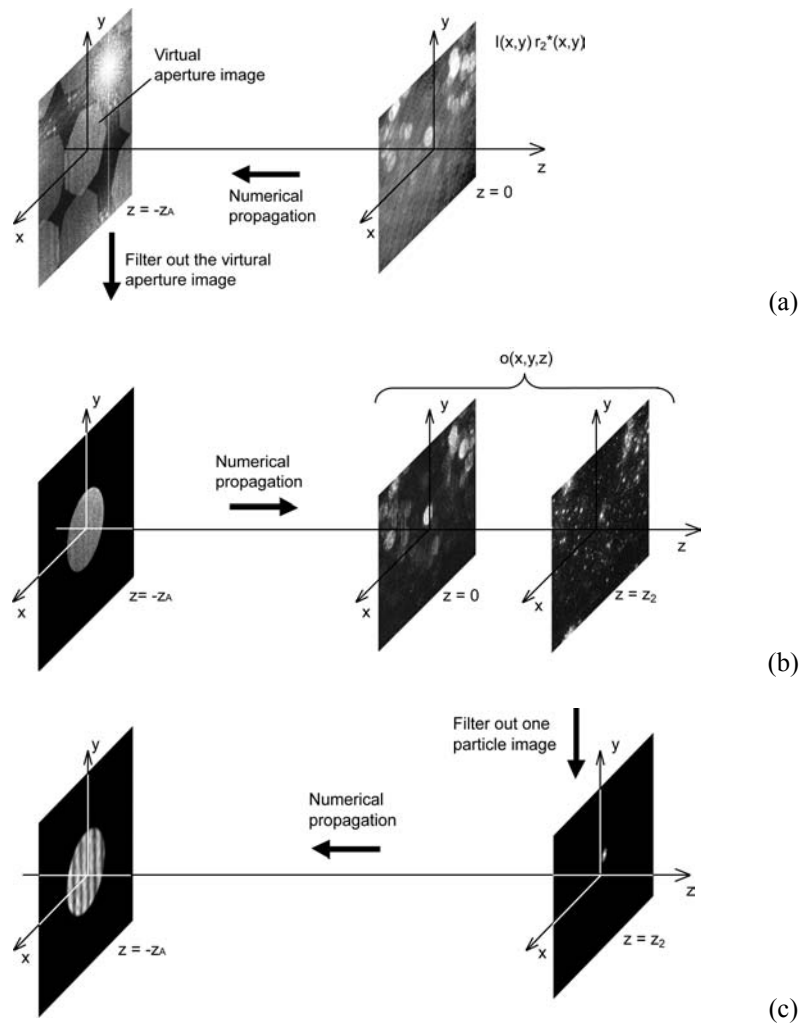

(a)

(b)

(c)

Figure 7: Schematic of the reconstruction process. a) The hologram is multiplied by $r*(x,y)$ and the resulting wave is propagated to the aperture plane; b) the virtual image is selected and propagated either to the recorded plane, where the images of the particles are defocused, or to the focused plane; c) a particle is selected and the wave is propagated again for calculating the particle size.

The recovering of the particle image is done in two steps because the reconstructed wavefield is calculated with a Fresnel approximation that imposes the condition that the longitudinal distances have to be larger than the transversal dimensions. For planes far enough from the hologram this condition is achieved. But the distance between the sensor plane and the focused plane is not large enough, thus propagating directly from the sensor will introduce errors in the calculated wavefield.

Figure 8 (a) and (b) shows the two reconstructed images in the sensor plane, where the images are defocused. Figure 8 (c) and (d) shows the focused images where pairs of glare points corresponding to the bubbles can be identified. In figure 8 (e) and (f) the bubbles have been numerated for allowing an easier identification in the subsequent analysis.

plane 1   plane 2

(a)   (b)

(c)   (d)

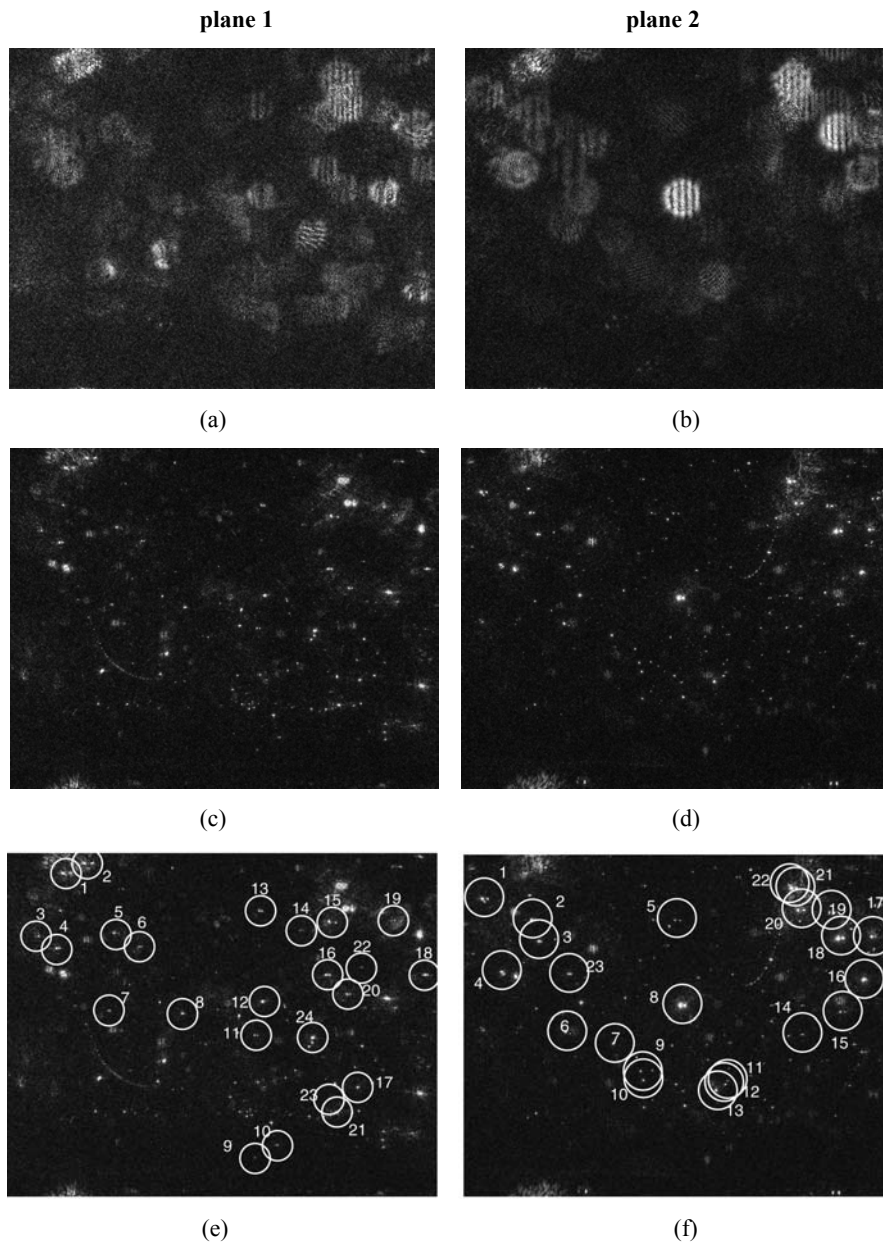(e)   (f)

Figure 8: Reconstructed images. Defocused images for plane 1 (a) and 2 (b) as they are imaged in the CCD sensor in the hologram recording. Focused images for plane 1 (c) and plane 2 (d). Bubble identification (e) and (f).

An important characteristic of the digital holography, common to the optical holography, is that any plane can be reconstructed. The first advantage, as already pointed out by Burke et al (2002), is that overlapping particles in the defocused plane can be separated in the focused plane, filtered out and propagated again to a defocused plane, where the final analysis for extracting the fringe frequency and, therefore the bubble diameter, can be done. An example of this capability is shown in figure 9. Bubbles #20, 21 and 22 that are overlapping in the original image (plane 2) are separated in the focused plane and can be analysed independently. Also bubble #23 is shown as an example of a good recovered image.

4. Size and velocity measurements

In the experiments presented in this work air bubbles were injected with a syringe in a cell filled with glycerine. The displacement of the bubbles when they were drifting freely to the surface has also been measured, applying the cross-correlation analysis to the focused images as it is done in a regular digital PIV experiment. Measured sizes and displacement are shown in figure 10. It can be seen that a wide range of sizes can be measured. The smaller bubbles are approximately 50 μm in diameter and the bigger are ~400 μm. In general bigger bubbles are located nearer the surface of the liquid and move faster towards the surface. Some other bubbles are still, floating inside the glycerine.
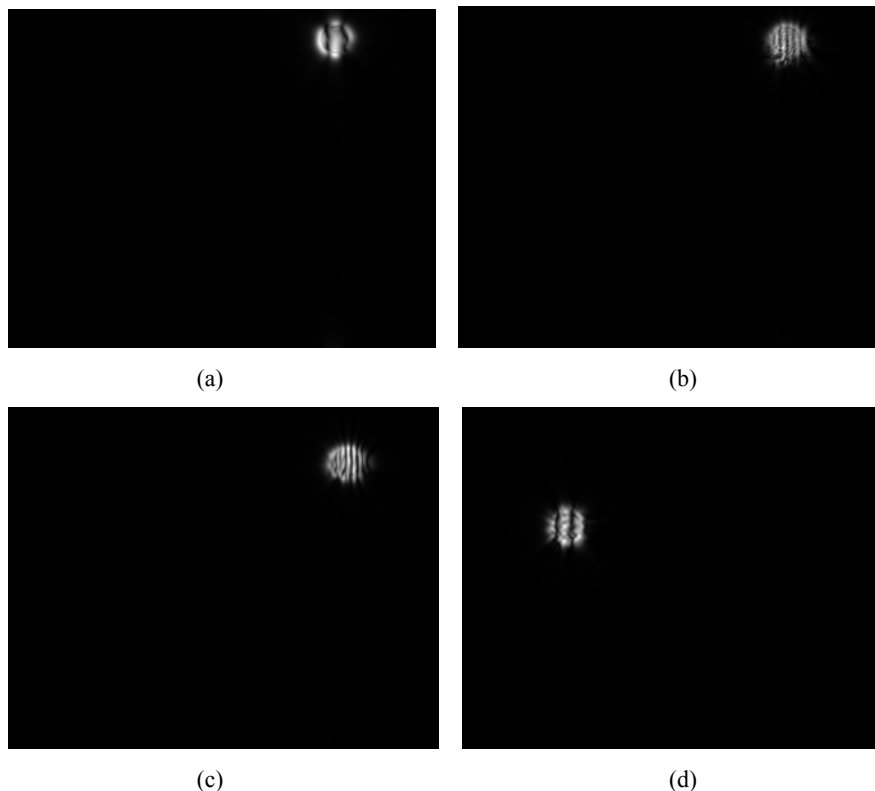

(a)

(b)

(c)

(d)

Figure 9: Independent reconstruction of overlapping particles in plane 2. Defocused images for bubbles (a) # 22 (diameter = 89 μm), (b) 21(211 μm), (c) 20 (266 μm) and (d) 23 (92 μm).
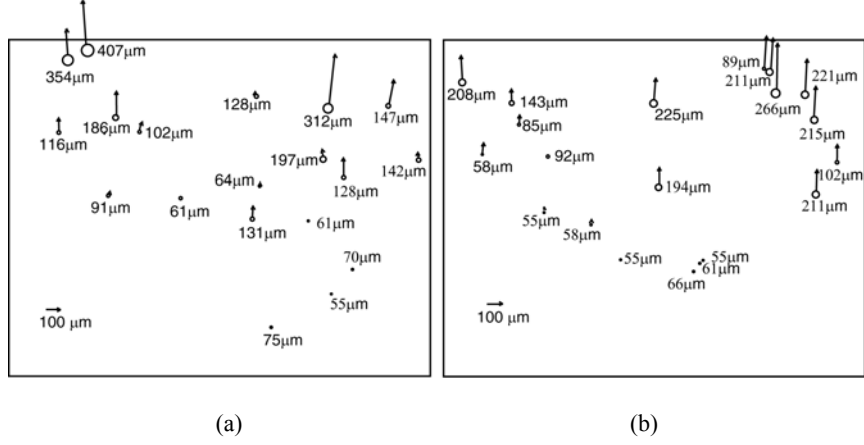
(a)	(b)

Figure 10: Bubble sizes and displacements measured in plane 1 (a) and 2 (b)

5. System limitations

It is also important to determine the limitations imposed by our recording system, such as the pixel size, the dimensions of the sensor, lens aperture, and so on. Let us first determine the smaller measurable diameter, which is determined by the aperture and the speckle size. The maximum angle subtended by the aperture ,σ' (figure 11) can be expressed as:

$$\tan\sigma' = \frac{\phi_a}{2(a'-\delta)} \qquad (7)$$

where ϕ_a is the diameter of the aperture, δ is the defocusing and a' is the image distance. The speckle size in the sensor plane is:

$$d_s = 1{,}22\frac{\lambda(a'-\delta)}{\phi_a} \qquad (8)$$
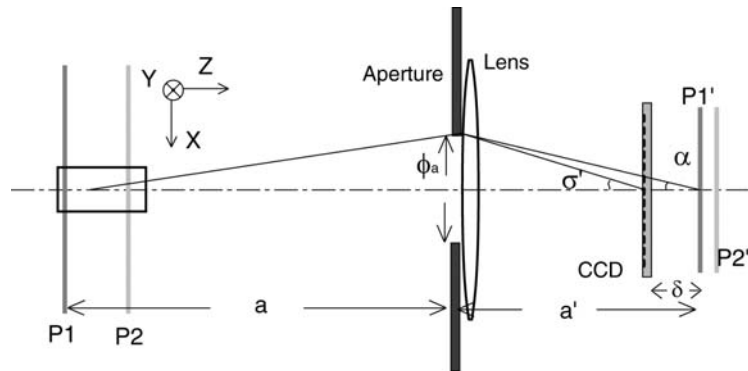

Figure 11: Recording system geometry

On the other hand, the minimum particle size corresponds to having only one fringe on the defocused particle image. Then

$$\tan\alpha = \frac{\phi_a}{2a'} = \Delta\varphi = \frac{\lambda}{D} \qquad (9)$$

9

Combining equations (7), (8) and (9) D can be written as:

$$D = \frac{d_s}{1,22} \frac{a'}{(a'-\delta)} \tag{10}$$

In DIPH the aperture has to be such that the speckle diameter in the recorded plane is three pixels ($d_s = 3d_{pix}$). Considering this the minimum measurable diameter will be:

$$d_{min} = 2.46 \frac{d_{pix}}{M \cos 45} \frac{a'}{(a'-\delta)} \tag{11}$$

being d_{pix} the pixel size and a' = f(1+M).

For d_{pix} = 6.7 μm, M=1, f= 120 mm and δ = 22,5 mm, the minimum diameter will be 25.9 μm. In our set-up with lower magnifications, the minimum bubble diameter will be 37.2 μm for plane 1 (δ = 22.5 mm, M = 0.71) and 35.5 μm for plane 2 (δ = 29.5 mm, M = 0.77). Smaller particle diameter can be measured increasing the system magnification, at the expense of reducing the measured region.

A solution for maintaining the visualized area and increasing the magnification would be by using a CCD camera with a larger sensor. For instance, commercial cameras with a CCD sensor of 4000x2670 pixels are now reasonably affordable and for the same conditions as the present case the minimum measurable particle diameter would be approximately 10 μm. A smaller pixel size will also reduce the minimum measurable diameter.

The condition for the maximum measurable diameter is a minimum fringe spacing of 6 pixels. Then, replacing Δφ in equation (5):

$$d_{max} = \frac{\lambda}{M \cos 45} \frac{\delta}{6d_{pix}} \tag{12}$$

This gives a maximum diameter of 600 μm for plane 1 (δ = 22.5 mm, M = 0.71) and 724 μm for plane 2 (δ = 29.5 mm, M = 0.77).

6. Conclusions

DIPH has been applied for the simultaneous measurement of the size and displacement of air bubbles in glycerine. Two planes have been simultaneously recorded but reconstructed independently. A new optical configuration for size measurement has been introduced. A mirror located after the fluid creates a new illuminating sheet, so the bubble field is measured with two laser sheets travelling in opposite directions. We have derived a new relation for diameter measurement for this configuration.

The system limitations have been analysed, establishing that the dynamic range of this configuration is quite large going from 30 μm up to several hundreds of microns.

References:

Burke J; Hess C; Kebbel V (2002), "Digital holography for whole field spray diagnostics", *11th International Symposium on Application of Laser Techniques to Fluids Mechanics*, Lisbon (Portugal), 8-11 July 2002.

Damaschke N; Nobach H; Tropea C (2001) "Global Phase Doppler Technique for Size and Velocity Measurements" *4th International Symposium on Particle Image Velocimetry*, Göttingen, Germany.

Glover A R; Skippon S M; Boyle R D (1995), "Interferometric laser imaging for droplet sizing: a method for droplet-size measurement in sparse spray systems", *Applied Optics*, Vol. 34, No. 36, 8409-8421.

Lobera L; Andrés N; Arroyo M P (2003), "From ESPI to Digital Image Plane Holography (DIPH): requirements, possibilities and limitations for velocity measurements in a 3-D volume", *EUROPIV 2 Workshop on Particle Image Velocimetry*, Zaragoza (Spain), March 2003.

Lobera J, Andrés N, Arroyo M P, (2004), "Digital speckle interferometry as a holographic velocimetry technique", *Meas. Sci. Technol.* 15, 718-724

Maeda M; Kawaguchi T; Hishida K (2000), Novel interferometric measurement of size and velocity distributions of spherical particles in fluid flows, Measurement Science and Technology, Vol 11, L13-L18.

Semidetnov N and Tropea C (2004), "Conversion relationships for multidimensional particle sizing techniques", *Meas. Sci. Technol.*,15, 112-118.